Journal of Alloys and Compounds, 207/208 (1994) 161–164
JALCOM 3030

The electronic properties of Ce in $CeFe_4P_{12}$

J. Simon Xue, Mark R. Antonio, Wesley T. White and L. Soderholm
Chemistry Division, Argonne National Laboratory, Argonne, IL 60439 (USA)

Susan M. Kauzlarich
Department of Chemistry, University of California, Davis, CA 95616 (USA)

Abstract

An investigation of the bonding behaviours of selected rare earth (R) containing filled skutterudite samples (RFe_4P_{12}) is reported. X-ray diffraction and magnetic properties of $CeFe_4P_{12}$ are compared with those previously published. The electronic structure and bonding properties of the R = La, Ce and Pr members of this series are probed by X-ray absorption near-edge spectroscopy (XANES), and compared with the L_3 edges of selected trivalent and tetravalent standards. We find that the Ce XANES is complex, indicating that although the Ce is primarily trivalent, there is evidence of complex electronic behaviour in $CeFe_4P_{12}$. A comparison of the L_3 edges of $LaFe_4P_{12}$, and $PrFe_4P_{12}$, as well as $CeFe_4P_{12}$, with those obtained from ionic model compounds reveals some bonding between the f-ion and the –FeP– framework in all cases.

1. Introduction

Although the compounds RFe_4P_{12} (R = La–Eu, Th, U) all form with the cubic filled-skutterudite structure [1–3], they exhibit widely different electronic behaviours. $LaFe_4P_{12}$ is superconducting below 4.1 K [4], and exhibits normal metallic conductivity above the critical temperature. Pr–Eu samples are also metallic, but not superconducting, and the R = Eu sample is ferromagnetic below 100 K [5]. In contrast, the R = U and Ce analogs are semiconductors [2]. The semiconducting behaviour, combined with the anomalously small cell constants of the Ce member of the RFe_4P_{12} series, led to the suggestion that Ce is tetravalent in $CeFe_4P_{12}$ [1]. Assuming the formulation $Ce^{4+}(Fe_4P_{12})^{4-}$, the Ce has a $4f^0$ configuration and therefore this sublattice should be diamagnetic. The polyanion $-(Fe_4P_{12})^{n-}-$ has previously been shown to contain exclusively low-spin Fe^{2+} [6] with filled t_{2g} orbitals, and therefore only a very small temperature independent paramagnetism (TIP). It is the $-(Fe_4P_{12})^{n-}-$ network that is expected to support conductivity, and because $-(FeP_3)^{4-}-$ is isoelectronic with the skutterudite CoP_3 [7], this sublattice is also expected to be behave like a diamagnetic semiconductor.

There are two independent reports on the paramagnetic behaviour of $CeFe_4P_{12}$ [2,8]. The samples exhibit temperature dependent susceptibilities, the magnitude of which appears to depend on details of the sample preparation [2]. The presence of an effective moment, presumably localized on Ce, raises questions about the appropriateness of the simplistic, ionic, electron-transfer model discussed above for $CeFe_4P_{12}$.

The X-ray absorption near edge structure (XANES) can be markedly sensitive to oxidation state. Furthermore, the single-ion nature of the probe, together with its fast (10^{-16} s) time scale make it an ideal tool to probe the rare earth valence and bonding in these filled-skutterudite materials. There is a measurable shift of the edge onset to higher energy with an increase in formal oxidation state. In addition, there are significant differences in the XANES region for data obtained from light rare earth ions with either the 3+ or 4+ oxidation state. R^{3+} ions in ionic solids have sharp, single peaks at their L_3 edge (white lines), corresponding to a transition from 2p to 5d localized states. For materials in which the R orbitals are hybridized, the sharp single peak is significantly broadened. In contrast, R^{4+} ionic systems, such as CeO_2, have two well defined transitions at the L_3-edge, and these transitions are not as sharp as those arising from R^{3+}. We have used this sensitivity of XANES to investigate the electronic character of Ce in $CeFe_4P_{12}$. We also compare our results with other R ion spectra, as well as other Ce spectra, to further understand the oxidation states and bonding of the R ion, and how this influences the bulk properties exhibited by the different members of the RFe_4P_{12} series.

SSDI 0925-8388(93)03030-M

2. Experimental section

Crystals of CeFe$_4$P$_{12}$ were synthesized using a tin flux method as outlined by [8]. Chips of Ce metal were made by cutting a Ce ingot in a nitrogen-filled glove box. These metal chips were combined with iron powder, red phosphorus and tin metal in the atomic ratio of Ce/Fe/P/Sn = 1:4:20:50. An evacuated quartz ampoule containing the reactants was quickly heated to 1100 °C for 10 h, in order to homogenize the melt, and then slow cooled at a rate of 6 °C/h to 650 °C. The tin flux was easily dissolved in hydrochloric acid (50%). The crystal yield using this method is about 78 wt%. X-Ray diffraction data were obtained either on single crystals using a Nicolet P3 with Mo radiation or on powders using a Scintag diffractometer, operating in the theta-theta geometry with Cu radiation.

DC magnetization measurements of CeFe$_4$P$_{12}$ were obtained using a SQUID magnetometer. Two samples, each about 100 mg of crystals, were measured in thin wall quartz sample holders. The field measurements, obtained at 5 K, show a linear field dependence over the measured range (0–5 T). The temperature dependence was measured from 10 to 280 K in an applied field of 500 Oe. The contribution from the sample holder was independently measured, and subtracted from the data. All data shown are corrected for diamagnetism [9].

XAFS were collected at ambient temperature on beam line X23-A2 at the National Synchrotron Light Source with a Si⟨311⟩ double crystal monochromator. The vertical slits were optimized to provide a total energy bandwidth of 0.8 eV for all three Ce L-edges.

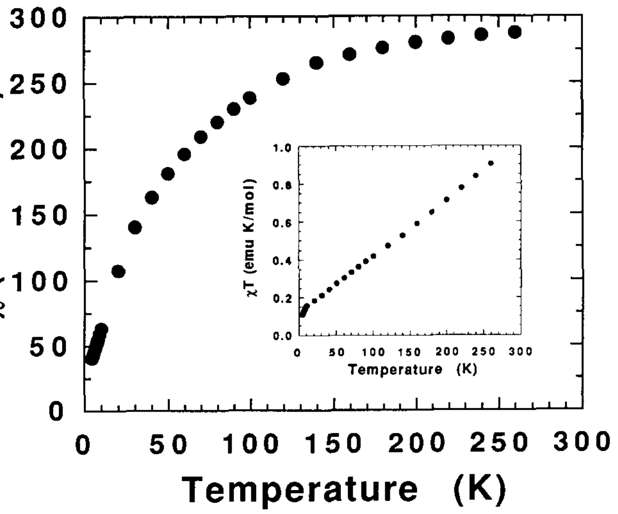

Fig. 1. Magnetic susceptibility data plotted as a Curie plot show a significant curvature. The inset shows the data replotted to account for the large temperature independent contribution. Data have been corrected for diamagnetism and the container contribution.

TABLE 1. Summary of the Lorentz contribution of the rare earth L$_3$ edge fitting obtained from EDGEFIT [11] (all data are convolved with a 2.0 eV Gaussian)

	Area	Height	Width (eV)	Energy (eV)
LaFe$_4$P$_{12}$	19.92	1.86	6.82	5484.3
La$_2$O$_3$	22.60	3.77	3.82	5484.3
CeFe$_4$P$_{12}$	13.78	1.10	8.00	5722.1
	1.07	0.14	4.74	5732.1
CeNT·6H$_2$O[a]	21.18	3.97	3.40	5721.7
CeTiO$_3$	18.86	2.44	4.92	5721.7
CeO$_2$	11.59	1.13	6.51	5725.7
	9.65	1.00	6.14	5733.4
PrFe$_4$P$_{12}$	18.80	1.56	7.69	5964.9
Pr$_6$O$_{11}$	18.00	1.54	7.42	5965.8
	5.29	0.51	6.56	5977.2
PrNT·nH$_2$O[a]	26.64	4.27	3.97	5965.4

[a] NT = (NO$_3$)$_3$.

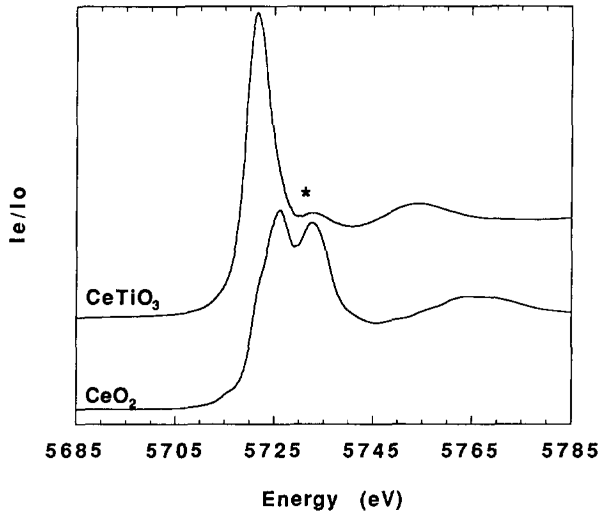

Fig. 2. Ce L$_3$ edge XANES for trivalent Ce (CeTiO$_3$) and tetravalent Ce (CeO$_2$) plotted to show the difference in edge energies, white lines, and number of edge peaks. These differences are used to assign oxidation state. The small peak indicated by an (*) in the CeTiO$_3$ data has been shown to arise from EXAFS [13], and is not electronic in origin.

The X-rays were detected using the electron yield technique [10] to obtain accurate edge resonance intensities and positions. With this configuration, the instrumental line broadening is significantly smaller than the broadening of about 3 eV caused by the natural lifetime of the L$_3$ or L$_2$ core hole. As a result, the XAFS shown here are not notably broadened by either instrumental effects or sample thickness. The three L-edge regions were scanned independently under the same experimental conditions with a step size of 0.25 eV/pt for the L$_{2,3}$ edges and 0.4 eV/pt for the L$_1$ edge. The scan-to-scan energy calibration was maintained to

0.2 eV. The L_3-edge XANES data are analyzed by conventional methods [11].

3. Results and discussion

The analyses of X-ray powder diffraction data from all $CeFe_4P_{12}$ samples are consistent with those previously published. All lines are indexable in the $Im3$ space group, and the cell constant, $a = 7.7839(4)$ Å does not vary significantly among the different sample preparations.

The temperature dependence of the magnetic susceptibility is shown as a Curie plot in Fig. 1. The data do not obey a simple Curie law, as evidenced by the significant curvature of the plot. The data are replotted to account for a temperature independent paramagnetism (TIP) according to

$$\chi T = C + \chi' T$$

where χ' is the TIP and C is the Curie constant. Fitting these data results in an effective moment of 1.00(2) μ_B per Ce ion and a temperature independent term of $\chi' = 3 \times 10^{-3}$ emu mol^{-1}. The measured effective moment is very similar to that previously reported [8]. This TIP is an order of magnitude larger than the 2.6×10^{-4} emu/mol reported previously [2], although the previous authors note a wide variation in the susceptibilities measured for different samples. Furthermore, this TIP is large considering that $CeFe_4P_{12}$ is semiconducting [2,8].

The bonding between the R ion and the $-(FeP_4)^{n-}-$ sublattice is often considered to be ionic in nature [3,12]. The R ion is argued to contribute either 3 or 4 electrons to the $-(FeP_4)^{n-}$- sublattice, and for the latter case, with low-spin Fe in which all the t_{2g} orbitals are filled, the sample should be a diamagnetic insulator. This sublattice would be analogous to the skutterudite CoP_3, which is a TIP semiconductor, with a corrected $\chi' = 7 \times 10^{-5}$ emu mol^{-1} [7]. The significantly larger χ' measured for the Ce analog, together with the temperature dependence to the observed magnetic susceptibility indicate that there is a problem with an electronic model involving complete electron transfer.

The L_3-edge XANES data are analyzed by curve fitting with Lorentz and arctangent functions, convolved with a 2-eV Gaussian broadening function [11], and the results are listed in Table 1. Representative Ce L_3 edge XANES of a Ce^{3+} and Ce^{4+} ion are shown in Fig. 2. By comparing the L_3 and L_1 edges, the small peak marked with an asterisk in the $CeTiO_3$ spectrum has been previously shown to be EXAFS, and not part of the single-ion XANES response [13]. The L_3 edge of the rare earth ion in $CeFe_4P_{12}$ is compared with the corresponding La and Pr XANES in Fig. 3. The La and Pr L_3 edge data are both sharp, single peaks, consistent with other results that have been used to assign these ions as trivalent. The Ce L_3 edge is more complex than those exhibited by La or Pr. The onset of the edge has an energy similar to that observed for $CeTiO_3$, indicating the presence of primarily Ce^{3+}. However, there is also a small peak at higher energy that is not due to EXAFS, but is instead electronic in origin. This peak is at a similar energy to that expected for a Ce^{4+} second peak, but it is much reduced in intensity. Furthermore, the Lorentzian height of the first peak is much reduced from that seen for either $CeTiO_3$ or $LaFe_4P_{12}$. The edge energy, combined with the reduced intensity of the white line and the indication of a second peak in the $CeFe_4P_{12}$ data lead us to conclude that there is some complex bonding between the Ce and the $-(FeP_4)^{n-}-$ sublattice. For example, these results are consistent with Ce d-orbital hybridization, as previously proposed to account for the behaviour of the Ce-analog [2].

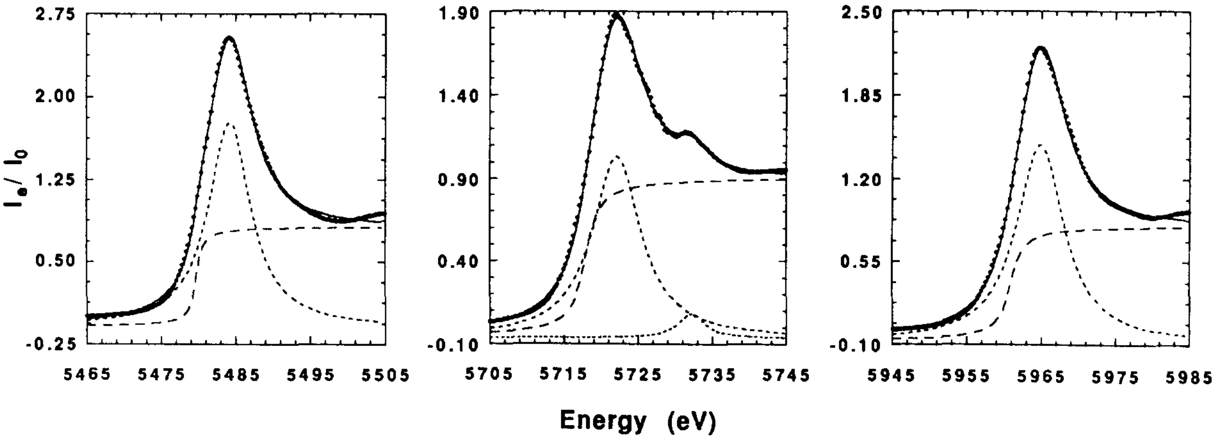

Fig. 3. The XANES data from (left) $LaFe_4P_{12}$, (middle) $CeFe_4P_{12}$ and (right) $PrFe_4P_{12}$. The Ce data show a significantly broadened white line, and the presence of a small second peak of electronic origin. The dotted lines show the fitted arctangent and Lorentzian contributions to the total, fitted, intensity (solid line).

A close look at the widths and areas obtained from a fit to the white lines of a variety of compounds shows that, even for La and Pr, which are considered to be ionic and trivalent, there is significant broadening to the observed transitions, indicating that there is some bonding even for these ions. This is consistent with the observation of superconductivity in the R = La filled-skutterudite analogs [4,14], because La^{3+} is diamagnetic, and therefore has no unpaired spins available to suppress superconductivity, even if there is some hybridization. On the other hand, $PrFe_4P_{12}$ has an f^2 configuration, and therefore magnetic density on the R site that can suppress superconductivity on the $-(FeP_4)^{n-}$- sublattice.

Acknowledgments

We thank F.W. Lytle and S.R. Wasserman for assistance with XANES data collection on X-23A2 at NSLS. This work is supported by the U.S. DOE, Basic Energy Sciences – Chemical Sciences, under contract W-31-109-ENG-38. One of us (WTT) received partial support from the Department of Educational Programs (ANL) through the Science and Engineering Research Semester program.

References

1 W. Jeitschko and D. Braun, *Acta. Crystallogr., Sect. B, 33* (1977) 3401.
2 G.P. Meisner, M.S. Torikachvili, K.N. Yang, M.B. Maple and R.P. Guertin, *J. Appl. Phys., 57(1)* (1985) 3073.
3 D.J. Braun and W. Jeitscho, *J. Less-Common Met., 76* (1980) 33.
4 G.P. Meisner, *Physica B, 108* (1981) 763.
5 A. Gerard, *J. Phys. C: Solid State, 16* (1983) 2797.
6 G.K. Shenoy, D.R. Noakes and G.P. Meisner, *J. Appl. Phys., 53(3)* (1982) 2628.
7 J. Ackermann and A. Wold, *J. Phys. Chem. Solids, 38* (1977) 1013.
8 F. Grandjean, A. Gerard, D.J. Braun and W. Jeitschko, *J. Phys. Chem. Solids, 45(8/9)* (1984) 877.
9 P.W. Selwood, *Magnetochemistry,* Interscience, New York, 1956, pp. 69–82.
10 F.W. Lytle, in H. Winick *et al.* (eds.), *Applications of Synchrotron Radiation*, Gordon and Breach, New York, 1989, p. 135.
11 F.W. Lytle, R.B. Greegor and E.C. Marques, *Proceedings 9th International Congress on Catalysis,* Calgary, Alta, Canada, The Chem. Inst. of Canada, 1986.
12 D. Jung, M.-H. Whangbo and S. Alvarez, *Inorg Chem., 29(12)* (1990) 2252.
13 J.E. Sunstrom, S.M. Kauzlarich and M.R. Antonio, *Chem. Mater., 5* (1993) 182.
14 G.P. Meisner, The superconductivity, structure, and magnetism of some ternary transition metal phosphides and arsenides, University of California, San Diego, 1982.